

**Enhanced tunnel magnetoresistance in a spinel oxide barrier with cation-site disorder**Hiroaki Sukegawa,<sup>1,\*</sup> Yoshio Miura,<sup>2</sup> Shingo Muramoto,<sup>2</sup> Seiji Mitani,<sup>1</sup> Tomohiko Niizeki,<sup>1</sup> Tadakatsu Ohkubo,<sup>1</sup> Kazutaka Abe,<sup>2</sup> Masafumi Shirai,<sup>2</sup> Koichiro Inomata,<sup>1</sup> and Kazuhiro Hono<sup>1</sup><sup>1</sup>National Institute for Materials Science (NIMS), 1-2-1 Sengen, Tsukuba 305-0047, Japan<sup>2</sup>Research Institute of Electrical Communication (RIEC) and Center for Spintronics Integrated Systems (CSIS), Tohoku University, Katahira 2-1-1, Aoba-ku, Sendai 980-8577, Japan

(Received 14 July 2012; published 2 November 2012)

We report enhanced tunnel magnetoresistance (TMR) ratios of 188% (308%) at room temperature and 328% (479%) at 15 K for cation-site-disordered  $\text{MgAl}_2\text{O}_4$ -barrier magnetic tunnel junctions (MTJs) with Fe ( $\text{Fe}_{0.5}\text{Co}_{0.5}$  alloy) electrodes, which exceed the TMR ratios theoretically calculated and experimentally observed for ordered spinel barriers. The enhancement of TMR ratios is attributed to the suppression of the so-called band-folding effect in ordered spinel MTJs [Phys. Rev. B **86**, 024426 (2012)]. First-principles calculations describe a dominant role of the oxygen sublattice for spin-dependent coherent tunneling, suggesting a mechanism of coherent tunneling occurring even in the disordered systems.

DOI: 10.1103/PhysRevB.86.184401

PACS number(s): 75.47.De, 72.25.Mk, 85.75.Dd

**I. INTRODUCTION**

The development of magnetic tunnel junctions (MTJs) with a large tunnel magnetoresistance (TMR) accelerated not only the practical application of spintronic devices, such as nonvolatile random access memories and read head sensors in hard disk drives, but also improved the understanding of spin-dependent transport phenomena. One of the breakthroughs regarding the TMR effect was the demonstration of giant TMR ( $\sim 200\%$ ) in Fe/MgO/Fe(001) and FeCo/MgO/FeCo(001) MTJs (Refs. 1 and 2) due to spin-dependent “coherent” tunneling in accordance with the theoretical prediction using first-principles calculation.<sup>3,4</sup> The  $\Delta_1$  Bloch state of Fe and of FeCo is fully spin polarized in the vicinity of Fermi energy  $E_F$  and couples with the  $\Delta_1$  evanescent state of MgO. The tunneling probability through the  $\Delta_1$  state dominates the total transport in the MTJ structure, leading to giant TMRs because of the half-metallicity of the  $\Delta_1$  state of Fe and FeCo for a wave vector normal to the plane, i.e., in-plane wave number  $k_{\parallel} = 0$ . Much larger TMR ratios have been reported for MgO-based MTJs with FeCoB, bcc-Co, and  $\text{Co}_2\text{FeAl}$  ferromagnetic electrodes<sup>5–8</sup> to date.

Recent investigations of a magnesium aluminate spinel ( $\text{MgAl}_2\text{O}_4$ ) ultrathin tunnel barrier with a normal spinel structure [space group:  $Fd\bar{3}m$ , Fig. 1(a)] as a candidate for an alternative coherent tunnel barrier material revealed relatively large TMR ratios of 117% at room temperature (RT) and 165% at 16 K for an epitaxial Fe/MgAl<sub>2</sub>O<sub>4</sub>/Fe(001) MTJ (Refs. 9 and 10). The  $\text{MgAl}_2\text{O}_4$  barrier is advantageous for a lattice-matched MTJ structure composed of typical bcc ferromagnetic materials, such as  $\text{Fe}_{1-x}\text{Co}_x$  alloys and Co-based Heusler alloys ( $\text{Co}_2\text{YZ}$ ) due to the small lattice mismatch ( $< 1\%$ ) between the  $\text{MgAl}_2\text{O}_4$  [ $a_{\text{spinel}} = 0.809$  nm (Ref. 11)] and the ferromagnetic alloys, leading to crystallographically coherent and dislocation-free barrier/electrode interfaces.<sup>9,12</sup> Unlike MgO,  $\text{MgAl}_2\text{O}_4$  is also a gemstone and chemically stable and, thus, nondeliquescent. However, a TMR ratio of 117% is rather small for perfectly lattice-matched MTJs suitable for coherent tunneling.<sup>13</sup> Although first-principles calculations predicted that the dominant conduction paths consist of the  $\Delta_1$  evanescent states of  $\text{MgAl}_2\text{O}_4$  in the coherent tunneling regime

as well as in the case of MgO(001) (Refs. 14 and 15), Miura *et al.*<sup>14</sup> theoretically revealed the absence of giant TMRs in  $\text{MgAl}_2\text{O}_4$  barriers; the  $\text{MgAl}_2\text{O}_4$   $\Delta_1$  evanescent states couple with not only the Fe majority spin  $\Delta_1$  states at  $k_{\parallel} = 0$ , but also the conductive channel of Fe minority-spin states resulting from a band-folding effect in the two-dimensional Brillouin zone of the in-plane wave vector ( $k_{\parallel}$ ) of Fe, which is formed by connecting the Fe lattice with the twice as large  $\text{MgAl}_2\text{O}_4$  lattice. Thus, the calculated upper limit for the TMR ratio of Fe/ $\text{MgAl}_2\text{O}_4$ (1.2 nm)/Fe is only 160%.

In this paper, we report that TMR ratios can be enhanced beyond the theoretical limit for MTJs with an  $\text{MgAl}_2\text{O}_4$  by introducing “cation-site disorder,” which effectively suppresses the band-folding effect limiting the TMR ratios. First-principles calculations show how coherent tunneling can occur through the  $\text{MgAl}_2\text{O}_4$  barrier even with cation-site disorder.

**II. EXPERIMENTS**

MTJ multilayers were deposited using magnetron sputtering with a base pressure of less than  $5 \times 10^{-7}$  Pa on MgO(001) single-crystal substrates. The Fe/ $\text{MgAl}_2\text{O}_4$ /Fe multilayers were Cr(40)/Fe(30)/Mg(0.40-0.45)/Mg-Al(0.90-1.5)/oxidation/Fe(7)/IrMn(12)/Ru(7) (thickness in nanometers). An MTJ with a structure of Cr(40)/Fe(30)/Fe<sub>50</sub>Co<sub>50</sub>(2.5)/Mg(0.40)/Mg-Al(0.90)/oxidation/Fe<sub>50</sub>Co<sub>50</sub>(2)/Fe(5)/IrMn(12)/Ru(7) was also prepared. To obtain better homogeneity of the Mg-Al composition in the  $\text{MgAl}_2\text{O}_4$  layer, an Mg-Al alloy layer was used, whereas, an Mg/Al bilayer was oxidized in the previous paper.<sup>9</sup> We prepared two Mg-Al targets with different compositions, and inductively coupled plasma analysis showed that the compositions of the deposited films were Mg<sub>40</sub>Al<sub>60</sub> (Mg rich) and Mg<sub>19</sub>Al<sub>81</sub> (Al rich). The barriers were formed using inductively coupled plasma oxidation in an Ar + O<sub>2</sub> atmosphere (6.0 Pa). After the deposition of each Fe layer, the multilayers were postannealed for 15 min *in situ* at 200 °C–350 °C to smooth their surfaces and to improve the (001) orientation. Postannealing was also performed at 500 °C after oxidation of the  $\text{MgAl}_2\text{O}_4$  layer. Finally, the multilayers were annealed at 175 °C under a magnetic field of 5 kOe for 30 min.

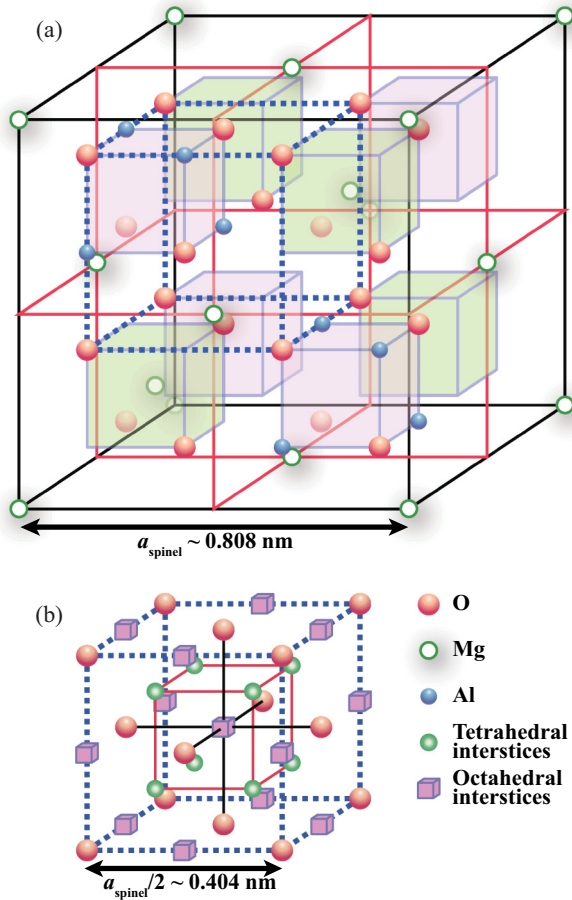


FIG. 1. (Color online) Schematics of (a) normal spinel  $MgAl_2O_4$  structure and (b) spinel structure with cation-site disorder (cation-disorder spinels).

High-resolution transmission electron microscopy (HRTEM) and nanoelectron beam diffraction (NBD) were used to investigate the microstructures of the barrier. The multilayers were then patterned into micrometer-scale junctions using a typical microfabrication technique, i.e., electron-beam lithography, photolithography, and Ar ion-beam etching. The MTJs were characterized using a dc four-probe method with a magnetic field applied in the  $Fe[100](\parallel MgO[110])$  direction.

### III. RESULTS AND DISCUSSION

Figures 2(a) and 2(b) show resistance-magnetic field ( $R$ - $H$ ) curves for an  $Fe/Mg(0.4)/Mg_{40}Al_{60}(0.9 \text{ nm})\text{-Ox}/Fe$  and an  $Fe/Mg(0.4)/Mg_{19}Al_{81}(0.9 \text{ nm})\text{-Ox}/Fe$  structure at RT and 15 K. The TMR ratios for the two structures were 185% at RT (328% at 15 K) and 188% at 300 K (304% at 15 K), respectively, which are much larger than those previously reported (117% at RT and 165% at 15 K).<sup>9</sup> The TMR ratios for both the Mg-rich and Al-rich MgAl-Ox-based MTJs were almost the same. This indicates that an epitaxial MgAl-Ox barrier can be formed using a wide range of Mg-Al compositions, meaning that the lattice constant of the barrier can be tuned by changing the Mg-Al composition. Furthermore, insertion of  $Fe_{50}Co_{50}$  layers between the Fe electrodes and the barrier

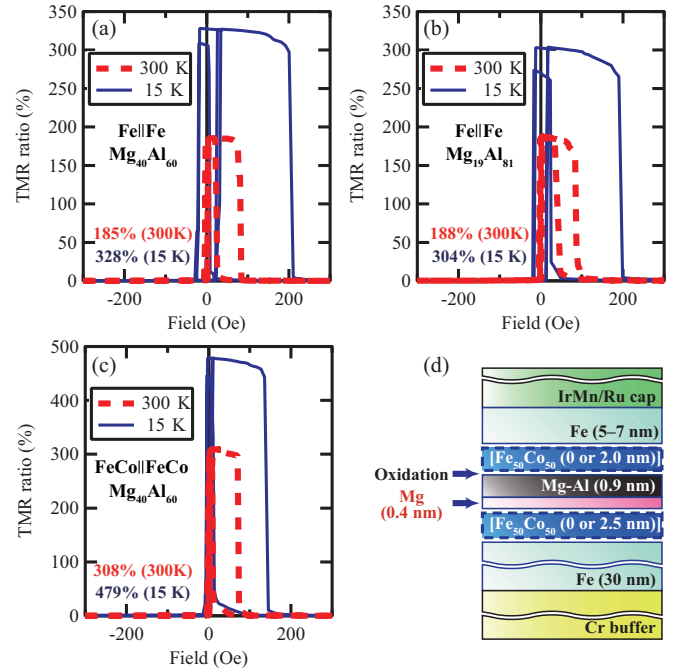


FIG. 2. (Color online) Resistance-magnetic-field curves for (a)  $Fe/Mg(0.4)/Mg_{40}Al_{60}(0.9 \text{ nm})\text{-Ox}/Fe$ , (b)  $Fe/Mg(0.4)/Mg_{19}Al_{81}(0.9 \text{ nm})\text{-Ox}/Fe$ , and (c)  $FeCo/Mg(0.4)/Mg_{40}Al_{60}(0.9 \text{ nm})\text{-Ox}/FeCo$  MTJs measured at RT (dotted lines) and 15 K (solid lines). (d) Schematic of MTJ stack.

greatly enhanced the TMR due to the larger spin polarization of FeCo in the coherent tunneling regime.<sup>2</sup> The TMR ratios reached 308% at RT and 479% at 15 K as shown in Fig. 2(c). The observed TMR ratios for our MTJs are comparable to those for MgO-based MTJs with FeCo(B)-based electrodes.<sup>2,7</sup>

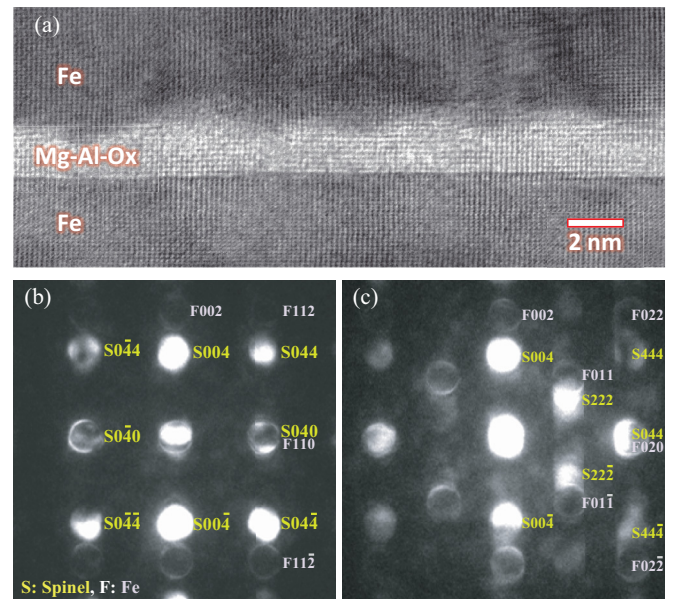


FIG. 3. (Color online) (a) Cross-sectional HRTEM image of  $Fe/Mg(0.45)/Mg_{40}Al_{60}(1.5 \text{ nm})\text{-Ox}/Fe$  MTJ in the  $Fe[110]$  direction. (b) and (c) Nanoelectron beam diffraction patterns around the barrier in (b)  $Fe[110]$  and (d)  $Fe[100]$  directions.

The large TMR ratios observed for conventional Fe and FeCo electrodes are evidence that coherent tunneling occurs in the MgAl<sub>2</sub>O<sub>4</sub> barrier, similar to MgO barriers. An MTJ stack is schematically illustrated in Fig. 2(d).

Figure 3(a) shows a cross-sectional HRTEM image of an Fe/Mg(0.45)/Mg<sub>40</sub>Al<sub>60</sub>(1.5 nm)-Ox/Fe MTJ in the Fe[110](||MgO substrate [100]) direction. The image shows a monocrystalline Fe/barrier/Fe structure with excellent lattice matching between the Fe and the barrier (mismatch ~0.5%). Figures 3(b) and 3(c) show NBD patterns (beam-spot size ~2 nm) around the barrier layer in the Fe[110] and Fe[100] directions, respectively. The patterns show that the barrier layer had a cubic structure and that the epitaxial relationship between the Fe and the barrier layers was Fe(001)[110]||MgAl<sub>2</sub>O<sub>4</sub>(001)[100]. However, there are few ordered spots for the spinel structure, {220}, {111}, and {311}. This suggested that the effective lattice repeat unit of the barrier was half that of a fully ordered spinel structure [Fig. 1(a)], meaning that the space group had changed.

Consideration of the cohesion mechanism of ionic spinels and rock-salt crystals led to the presumption that the reduction in the unit-cell size occurs due to cation-site disordering. Since

the conventional Mg<sup>2+</sup>-Al<sup>3+</sup> site exchange (transformation from normal to inverse spinel) does not affect the unit-cell size and its space group, cations must occupy vacant octahedral and tetrahedral sites surrounded by anions (O<sup>2-</sup>) as shown in Fig. 1(b). In this case, the space group of the spinel changes from *Fd*3̄*m* to either *Fm*3̄*m* or *F*43*m* due to the disordering. There are five candidates for the cation-disordered spinel structure.<sup>16</sup> Taking into account the dynamical effect in the NBD intensity analysis, we identified the defective rock-salt and all-interstices models of Sickafus<sup>16</sup> as possible structures. The reason for the formation of the nonequilibrium “cation-disorder spinel” structure is that the oxidation and postannealing processes were carried out at temperatures much lower than the melting point of MgAl<sub>2</sub>O<sub>4</sub> (~2122 °C). In addition, the formation of a large number of antiphase boundaries (APBs) in an ultrathin barrier could effectively create the cation-disorder spinel structure since the APBs inhibit long-range cation-site ordering of the spinel structure. For the Fe<sub>3</sub>O<sub>4</sub> thin film with an (inverse) spinel structure, as the film becomes thinner, the APB volume fraction increases, and the film resistivity increases rapidly.<sup>17</sup> The lattice spacing in the in-plane direction of Fe[220] was determined to be 0.2039 nm

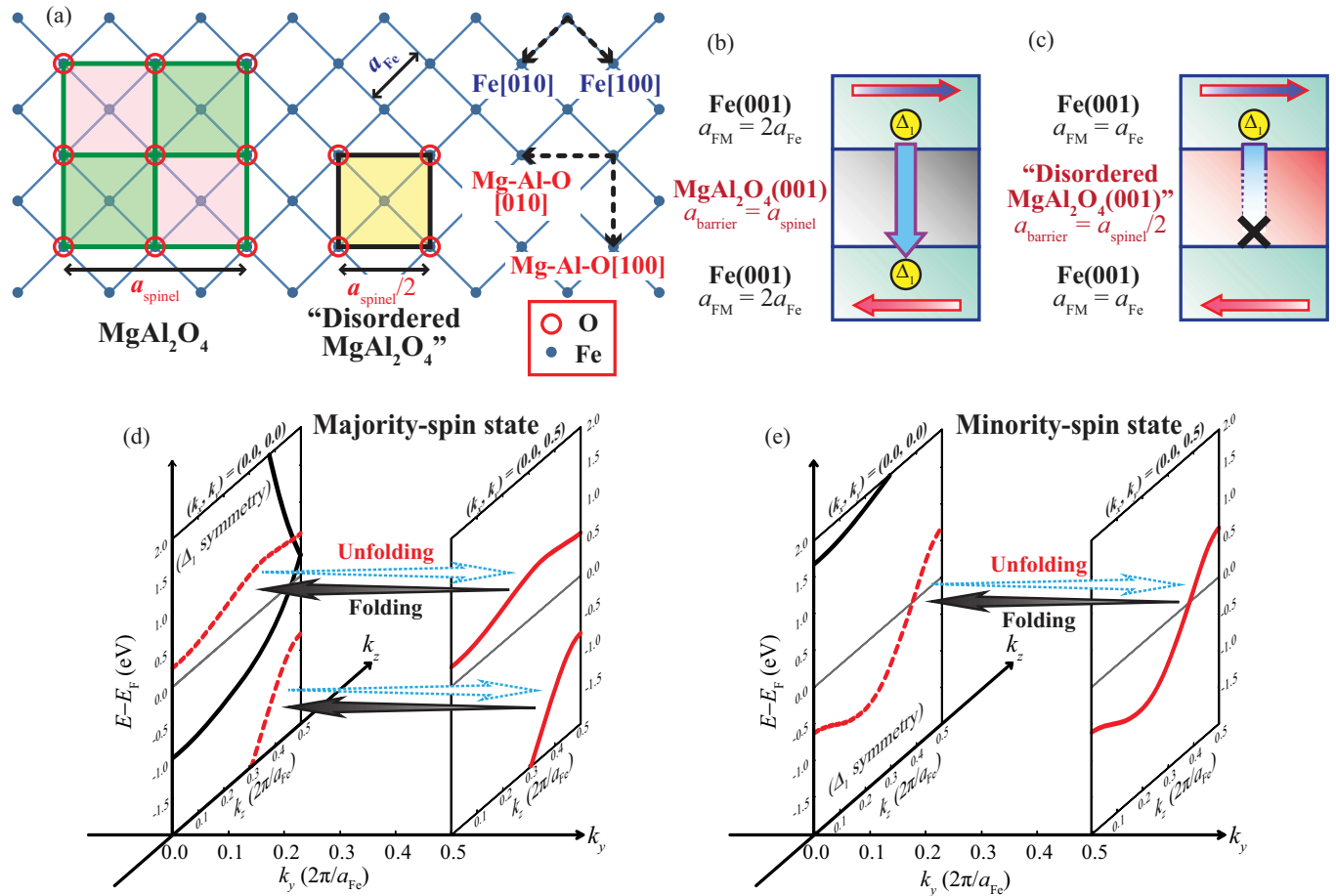


FIG. 4. (Color online) (a) Epitaxial relationships between MgAl<sub>2</sub>O<sub>4</sub> and Fe layers. (b) and (c) Schematics of transport through  $\Delta_1$  states for Fe/MgAl<sub>2</sub>O<sub>4</sub>/Fe with (c) ordered and (d) disordered spinel barriers for an antiparallel configuration;  $a_{\text{FM}}$  indicates an effective in-plane unit cell of ferromagnetic electrodes for each stack. (d) and (e) Schematics of band-folding and band-unfolding effects of Fe electrodes for (d) majority-spin band and (d) minority-spin band of Fe. Solid lines indicate primitive band dispersions of Fe- $\Delta_1$ . Dashed lines indicate folded band dispersions when  $a_{\text{barrier}} = a_{\text{spinel}}$ .

by x-ray diffraction. Using the lattice spacing of Fe and the mismatch determined by HRTEM (0.5%), we calculated the lattice constant of the cation-disorder  $\text{MgAl}_2\text{O}_4$  to be 0.410 nm.

An ordered spinel structure was previously observed for  $\text{Fe/MgAl}_2\text{O}_4/\text{Fe}$  stacking through NBD analysis (i.e.,  $\{220\}$  spots were clearly observed in the barrier and, thus,  $a_{\text{barrier}} = a_{\text{spinel}}$ ).<sup>9</sup> The moderate TMR ratio of 165% at 16 K is consistent with the first-principles calculation for ordered spinels.<sup>14</sup> In contrast to the previous observation, we have now observed a much larger TMR ratio (328% at 15 K) for  $\text{Fe/MgAl}_2\text{O}_4/\text{Fe}$  with a cation-disorder spinel barrier with a unit-cell size of half that of a primitive  $\text{MgAl}_2\text{O}_4$  structure (i.e.,  $a_{\text{barrier}} = a_{\text{spinel}}/2$ ) [see Fig. 4(a)], corresponding to the unfolding case of Fe band dispersion. To visualize the TMR change due to the band-folding effect, we prepared schematics of transport through the  $\Delta_1$  states for an  $\text{Fe/MgAl}_2\text{O}_4/\text{Fe}$  structure with an ordered or disordered spinel barrier [Figs. 4(b) and 4(c), respectively]. Figures 4(d) and 4(e) schematically show the band-folding and band-unfolding effects for the majority- and minority-spin bands of Fe electrodes. In these figures, the  $z$  direction is perpendicular to the film plane, and calculated band dispersions with  $\Delta_1$  symmetry are displayed. When the  $\text{MgAl}_2\text{O}_4$  is fully ordered ( $a_{\text{barrier}} = a_{\text{spinel}}$ ), the corresponding in-plane unit-cell size of Fe ( $a_{\text{FM}}$ ) is  $2a_{\text{Fe}}$  [Fig. 4(b)]. In this situation, the Fe dispersion for  $(k_x, k_y) = (0.0, 0.5)(\frac{2\pi}{a_{\text{Fe}}})$  (red solid curve) is folded to  $k_{\parallel} = (k_x, k_y) = (0.0, 0.0)$  (red dashed curve) due to the reduced two-dimensional Brillouin zone of Fe (new zone boundary:  $k_y/\frac{2\pi}{a_{\text{Fe}}} = 0.25$ ), causing new conductive channels coupled to the  $\Delta_1$  evanescent state of the  $\text{MgAl}_2\text{O}_4$  to open (band folding).<sup>18</sup> The new channel for the minority-spin band destroys the half-metallicity of the  $\Delta_1$  states in Fe/ordered- $\text{MgAl}_2\text{O}_4/\text{Fe}(001)$  MTJs [Fig. 4(e)], leading to a considerable reduction in the TMR ratio. This means that transport through the new channels can be suppressed by reducing the lattice constant of the  $\text{MgAl}_2\text{O}_4$  barrier ( $a_{\text{barrier}} = a_{\text{spinel}}/2$ ), i.e., by unfolding the band dispersions (band unfolding). The TMR enhancement in the present MTJs is, thus, attributed to coherent tunneling between the unfolded  $\Delta_1$  states in Fe electrodes through the  $\Delta_1$  states in the cation-disorder spinel barrier as shown in Fig. 4(c). Consequently, the TMR ratio for even  $\text{MgAl}_2\text{O}_4$ -based MTJs should be large if the Brillouin zone of Fe is effectively prevented from folding by introducing appropriate disordering into the barrier.

This finding of “disorder-induced” TMR enhancement is important for understanding the spin-dependent coherent tunneling phenomenon because site disordering has generally been regarded as undesirable for coherent spin transport. Even though cation-site disordering was observed in the barrier, as discussed above, there was almost perfect lattice matching between the barrier and the electrodes, there was good crystallinity with high (001) orientation, and there were atomically flat interfaces, ensuring coherent tunneling in the MTJs. Note that the clear difference in the TMR ratio between  $\text{Fe/MgAl}_2\text{O}_4/\text{Fe}$  MTJs with ordered and with disordered spinel barriers completes an experimental demonstration of the effect of band folding described theoretically by Miura *et al.*<sup>14</sup>

Using first-principles electronic structure and transport calculations, we investigated how the cation-site disorder may affect the coherence of electron tunneling. For

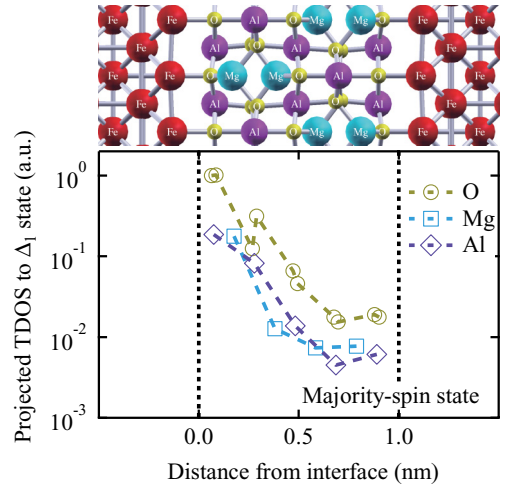


FIG. 5. (Color online) Projected tunneling density of states (TDOS) for  $\Delta_1$  states of O, Mg, and Al sites for majority-spin electrons as a function of distance from the  $\text{Fe/MgAl}_2\text{O}_4$  interface.

the electronic structure calculations, we used a supercell  $\text{Fe/MgAl}_2\text{O}_4/\text{Fe}(001)$  MTJ containing 11 atomic layers of bcc Fe and 9 atomic layers of  $\text{MgAl}_2\text{O}_4$ . The in-plane lattice parameter was set to 0.5733 nm ( $=2a_{\text{Fe}}$ ). The calculation process and the related results are described in detail in Ref. 14. Figure 5 shows the TDOS for the  $\Delta_1$  states of O, Mg, and Al sites for majority-spin electrons as a function of the distance from the  $\text{Fe/MgAl}_2\text{O}_4$  interface. The magnitude of the projected TDOS for oxygen was doubled since two equivalent oxygen atoms were the same distance from the interface. The projected TDOS for oxygen was several times larger than those for Mg and Al. This means that the  $\Delta_1$  electrons traveling from one to the other Fe electrode propagate mainly through the oxygen fcc sublattice, so cation-site disorder has little effect on coherent tunneling in  $\text{Fe/MgAl}_2\text{O}_4/\text{Fe}$  MTJs.

#### IV. CONCLUSIONS

We have demonstrated enhancement of TMR in MTJs with an  $\text{MgAl}_2\text{O}_4$  barrier by introducing cation-site disorder in which the observed TMR ratios up to 479% at 15 K are much larger than the value theoretically calculated for ordered spinel MTJs. This is attributed to the suppression of the so-called band-folding effect in ordered spinel MTJs. First-principles calculations suggest a mechanism of coherent tunneling in the disordered system: The  $\Delta_1$  states in the oxygen fcc sublattice are presumably a dominant conduction path for coherent tunneling. The present paper demonstrates an alternative material to MgO for giant TMRs due to coherent tunneling as well as experimental evidence for the folding effect in the coherent tunneling regime.

#### ACKNOWLEDGMENTS

This work was partly supported by KAKENHI (Grants No. 22686066, No. 23246006, No. 22360014, and No. 22760003) from the Japanese Ministry of Education, Culture, Sports, Science and Technology.

\*sukegawa.hiroaki@nims.go.jp

- <sup>1</sup>S. Yuasa, T. Nagahama, A. Fukushima, Y. Suzuki, and K. Ando, *Nat. Mater.* **3**, 868 (2004).
- <sup>2</sup>S. S. P. Parkin, C. Kaiser, A. Panchula, P. M. Rice, B. Hughes, M. Samant, and S.-H. Yang, *Nat. Mater.* **3**, 862 (2004).
- <sup>3</sup>W. H. Butler, X.-G. Zhang, T. C. Schulthess, and J. M. MacLaren, *Phys. Rev. B* **63**, 054416 (2001).
- <sup>4</sup>J. Mathon and A. Umerski, *Phys. Rev. B* **63**, 220403(R) (2001).
- <sup>5</sup>S. Ikeda, J. Hayakawa, Y. Ashizawa, Y. M. Lee, K. Miura, H. Hasegawa, M. Tsunoda, F. Matsukura, and H. Ohno, *Appl. Phys. Lett.* **93**, 082508 (2008).
- <sup>6</sup>S. Yuasa, A. Fukushima, H. Kubota, Y. Suzuki, and K. Ando, *Appl. Phys. Lett.* **89**, 042505 (2006).
- <sup>7</sup>Y. M. Lee, J. Hayakawa, S. Ikeda, F. Matsukura, and H. Ohno, *Appl. Phys. Lett.* **89**, 042506 (2006).
- <sup>8</sup>W. H. Wang, E. Liu, M. Kodzuka, H. Sukegawa, M. Wojcik, E. Jedryka, G. H. Wu, K. Inomata, S. Mitani, and K. Hono, *Phys. Rev. B* **81**, 140402(R) (2010).
- <sup>9</sup>H. Sukegawa, H. Xiu, T. Ohkubo, T. Furubayashi, T. Niizeki, W. H. Wang, S. Kasai, S. Mitani, K. Inomata, and K. Hono, *Appl. Phys. Lett.* **96**, 212505 (2010).
- <sup>10</sup>H. Sukegawa, H. Xiu, T. Ohkubo, T. Niizeki, S. Kasai, T. Furubayashi, S. Mitani, K. Inomata, and K. Hono, *J. Magn. Soc. Jpn.* **35**, 254 (2011).
- <sup>11</sup>K. E. Sickafus and J. M. Wills, *J. Am. Ceram. Soc.* **82**, 3279 (1999).
- <sup>12</sup>R. Shan, H. Sukegawa, W. H. Wang, M. Kodzuka, T. Furubayashi, T. Ohkubo, S. Mitani, K. Inomata, and K. Hono, *Phys. Rev. Lett.* **102**, 246601 (2009).
- <sup>13</sup>Although Shan *et al.* (Ref. 12) were the first to obtain an epitaxial MgAl<sub>2</sub>O<sub>4</sub> barrier, the TMR enhancement by coherent tunneling through the barrier was negligibly small due to inadequate postannealing. Fe/MgAl<sub>2</sub>O<sub>4</sub>/Fe MTJs fabricated under the same postannealing conditions had a TMR ratio of only 40%–58% at RT.<sup>10</sup>
- <sup>14</sup>Y. Miura, S. Muramoto, K. Abe, and M. Shirai, *Phys. Rev. B* **86**, 024426 (2012).
- <sup>15</sup>J. Zhang, X.-G. Zhang, and X. F. Han, *Appl. Phys. Lett.* **100**, 222401 (2012).
- <sup>16</sup>K. E. Sickafus, *J. Nucl. Mater.* **312**, 111 (2003).
- <sup>17</sup>W. Eerenstein, T. T. M. Palstra, T. Hibma, and S. Celotto, *Phys. Rev. B* **66**, 201101(R) (2002).
- <sup>18</sup>New conductive channels in minority-spin states always present at  $k_{\parallel} = 0$  of Fe if a doubled in-plane unit cell is used in the Fe/MgO/Fe(001) structure. However, band folding occurs also in the MgO regions in the doubled unit-cell geometry of the structure, and the folded Fe and MgO states are labeled as different  $k_{\parallel}$ 's compared with the unfolded states. Thus, the folded Fe channels at  $k_{\parallel} = 0$  never couple with the  $\Delta_1$  evanescent state in the MgO, the same as with the primitive unit cell. In the case of Fe/MgAl<sub>2</sub>O<sub>4</sub>/Fe(001), band folding occurs only in the Fe electrode (the MgAl<sub>2</sub>O<sub>4</sub> bands are not folded). This changes the periodic boundary condition of the system in the in-plane direction, and the new folded Fe channels at  $k_{\parallel} = 0$  can couple with the  $\Delta_1$  evanescent state in the MgAl<sub>2</sub>O<sub>4</sub>.